DEVELOPMENT OF DEXAMETHASONE-LOADED POLY(ε-CAPROLACTONE)/SNPS BIOCOMPOSITE MATERIALS USING SUPERCRITICAL CARBON DIOXIDE PROCESSES

Maria B.C. de Matos[1], Ana P. Piedade[2], Carmen Alvarez-Lorenzo[3], Angél Concheiro[3], Mara E.M. Braga[1], Hermínio C. de Sousa[1*]

[1]CIEPQPF, Chemical Engineering Department
FCTUC, University of Coimbra
Rua Sílvio Lima, Pólo II – Pinhal de Marrocos, 3030-790 Coimbra, Portugal

[2]CEMUC, Mechanical Engineering Department
FCTUC, University of Coimbra
Rua Luís Reis Santos, Pólo II – Pinhal de Marrocos, 3030-788 Coimbra, Portugal

[3]Departamento de Farmacia y Tecnología Farmacéutica, Facultad de Farmacia
Universidad de Santiago de Compostela
15782-Santiago de Compostela, Spain

Email: hsousa@eq.uc.pt

Abstract. Biodegradable polymeric scaffolds with suitable morphological and mechanical properties are known to be useful for several biomedical and hard-tissue engineering applications. Moreover, the combination of biocompatible polymers with silica nanoparticles (SNPs) and bioactive substances may lead to nanocomposite materials having enhanced physical and biological properties for the above referred applications. This work reports the development of dexamethasone (DXMT)-loaded biocomposites that were prepared with poly(ε-caprolactone) (PCL) and with mesoporous MCM-41 SNPs and by using supercritical carbon dioxide ($scCO_2$) processes, namely $scCO_2$-assisted foaming/mixing and scCO2 deposition of bioactive substances. Pure PCL and PCL/MCM-41 composite materials (90:10 and 70:30, wt.%) were processed by $scCO_2$ foaming/mixing at different experimental density (801.4 and 901.2 kg/m^3), processing time (2 and 14 hours) and depressurization (0.2 and 3.0 dm^3/min) conditions. Additionally, mesoporous MCM-41 and SBA-15 SNPs were loaded with DXMT using a $scCO_2$ deposition method and later incorporated into DXMT/PCL physical mixtures using the previously employed $scCO_2$-assisted foaming/mixing method and at the aforementioned experimental conditions. All prepared materials were characterized by FTIR, mercury intrusion porosimetry, helium pycnometry, nitrogen adsorption, simultaneous differential thermal analysis (SDT) and scanning electron microscopy (SEM). Drug release studies were performed in order to evaluate and to compare DXMT release profiles. Results indicated that biocomposites physical and morphological properties were strongly dependent on the employed processing conditions. In addition, in vitro DXMT release experiments presented quite distinct release profiles, which were also dependent on the employed experimental foaming/mixing operational conditions as well as on the relative composition of previously DXMT-loaded SNPs. In conclusion, these results demonstrated the viability of using $scCO_2$ deposition and foaming/mixing methods for the development of DXMT-loaded PCL/SNPs biocomposite materials that present advantageous properties for hard-tissue engineering applications.

Keywords: Supercritical carbon dioxide, foaming/mixing, drug deposition, poly(ε-caprolactone), dexamethasone, mesoporous silica nanoparticles.

1. Introduction

Many techniques allow the conventional production of porous scaffolds, however when the incorporation of bioactive additives is intended, these methods make use of organic solvents/chemicals, which must be removed by additional extraction/purification steps, and/or use high temperatures that may induce drug thermal/chemical degradation [1].

Supercritical fluids (SCF), namely supercritical carbon dioxide ($scCO_2$), have emerged as "green" routes to overcome the drawbacks of conventional techniques [1, 2, 3]. Adequate porosity and pore sizes may be created controlling process parameters. Upon depressurization, when the polymer phase is supersaturated with CO_2, thermodynamic instability occurs, and the gas leaves the polymer phase occurring gas bubble nucleation. This nucleation stage involves the assembling of CO_2 molecules, with concurrent homogeneous and heterogeneous nucleation mechanisms occurring upon phase separation of the polymer–CO_2 solution [4]. Moreover, the use of $scCO_2$ as mobile phase can facilitate the diffusion of an additive and improve its incorporation rate in inorganic matrixes [5] and in previously processed polymeric or composites material [6], as well as simultaneous preparation of 3D structures and the incorporation of additives at mild processing conditions [7], avoiding several steps in the production of these materials that characterize conventional techniques.

The main objective of this work was the development and characterization of composite foams and the incorporation during processing of a model bioactive molecule widely used drug in osteogenic media to improve stem cell differentiation towards the osteogenic lineage [8, 9]. Thus, $scCO_2$ was used as a foaming agent at mild processing conditions to control poly(ε-caprolactone) PCL and PCL/silica nanoparticles (SNPs) composite foam characteristics, and to incorporate dexamethasone (DXMT) into the melted polymer.

2. Materials and Methods

2.1 Chemicals

The PCL pellets (M_w of 45000 Da), dexamethasone (purity 98%), methanol, acetone and mesoporous silica nanoparticles MCM-41 (pore volume 0.98 cm^3/g and 2.3-2.7 nm of pore size, surface area of 1000 m^2/g) were supplied by Sigma-Aldrich. SBA-15 SNPs were provided by ClaytecInc (average BJH Framework Pore Size 8.5 nm, total pore volume 0.93 cm^3/g, surface area 718 m^2/g). Panreac supplied ethanol (99.5% purity). CO_2 was obtained from Praxair with purity of 99.998%. Dialysis membranes (molecular weight cut-off of 8000 Da) and clamps were supplied by Spectrum Laboratories.

2.2 Experimental Procedure

Polymer preparation. PCL was dissolved in acetone and precipitated in methanol and water to acquire the powder form. Samples were centrifuged, dried and stored. PCL powders and MCM-41 SNPs were physically mixed (90:10 and 70:30, wt.%) in glass vials.

$scCO_2$-assisted foaming. Experimental conditions were varied based on literature [2, 3, 4, 9] and $scCO_2$ properties in order to optimize SCF foaming. PCL and MCM-41 SNPs were physically mixed in a glass vial prior to $scCO_2$-assisted foaming and then introduced in the high pressure cell. Thus, for the same temperature (35ºC), two pressures and two different proportions of PCL:MCM-41 were studied: 14.0 MPa and 25.0 MPa (0.801 and 0.901 g/cm^3, correspondingly), 70:30%wt and 90:10%wt, respectively. Also, for each parameter previously mentioned, the process time and depressurization rate were varied: 2 and 14 h and 0.2 and 3.0 dm^3/min, respectively. Moreover, control samples were processed for the same conditions where PCL:MCM-41 ratio was 100:0. All the assays were performed in duplicate.

$scCO_2$ deposition and mixing. DXMT was loaded into pure mesoporous MCM-41 and SBA-15 SNPs by $scCO_2$ impregnation/deposition, at the previously mentioned pressures and temperature, for 2h and 14 h with depressurization rate of 0.2 L/min. SNPs were placed into sealed dialysis membranes and then introduced in a high pressure view-cell which was previously loaded with DXMT. DXMT-loaded SNPs were then incorporated into 2%wt DXMT/PCL physical mixtures using $scCO_2$-assisted foaming at the previously mentioned pressures and temperature, for 14 h and 0.2 dm^3/min. Physical mixtures PCL/DXMT were also foamed.

2.3 Characterization

FTIR-ATR spectroscopy measurements were performed on a Jasco FTIR spectrometer (Infrared Spectrum, Jasco, 4200 type A) using the Attenuated Total Reflectance (ATR) technique. The spectra were obtained at a 4 cm^{-1} resolution, 256 scans and processed by Jasco Spectra Analysis.

Thermal behavior of PCL-pellet, PCL-powder and $scCO_2$ processed material was determined on a Simultaneous Differential Thermal equipment (TA Q600) using standard alumina pans. Measurements were made on samples of 7-11 mg in the temperature range between 25 and 700 ºC at a heating rate of 2 ºC/min. The instrument was calibrated with indium. Mass loss, characteristic temperatures and enthalpies were calculated using the software TA Universal Analysis. The results are the average and standard deviation of two samples.

PCL and composites crystalline phases were compared before and after foaming experiments using a Philips X'Pert diffractometer with Co radiation ($\lambda_{K\alpha1}$ = 0,178896 nm and $\lambda_{K\alpha2}$ = 0,179285 nm). 2θ values were varied from 6º up to 60º. Acquisition step was 0.004º and acquisition time was 1s/step (40kV and 35mA).

Average pore diameter, pore volume and surface area were determined by nitrogen adsorption using a ASAP 2000 Micromeritics, model 20Q-34001-01. Surface area was determined by the BET method, pore volume and average pore diameter were calculated using BJH method. Pore size distribution, total pore volume and porosity were determined by mercury intrusion. Apparent and bulk densities were also determined by this method using Autopore IV 9500 Micromeritics. The density of the foams was measured by helium picnometry (Quanta-Chrome, MPY-2). The results are the average and standard deviation of two samples.

The $scCO_2$-foamed samples were analyzed for compression employing a texture analyzer (TA.XT plus). The analytical probe (P/10, 1 cm diameter) compressed each sample at a 1 mm/s rate and at a 3 mm depth. Employed activation force was 5 gf and the parameters were determined at 10% strain.

Samples were freeze-fractured in liquid nitrogen and the obtained cross-sections were examined by SEM (Philips XL30, 10kV), after gold-sputtering for 25s. SNPs presence was confirmed by image analysis of backscattered electrons and by EDX.

Drug sorption studies were performed in order to determine the drug loading ability of MCM-41 and SBA-15 in conventional liquid solvents. Thus, MCM-41 and SBA-15 was immersed into different dexamethasone solutions: aqueous and ethanolic solutions (26 g/ml). At predetermined time intervals up to 72h, an aliquot of the liquid media was read in a UV-Vis spectrophotometer (Jasco, Model V650, Japan).

Drug release assays from loaded SNPs, PCL and composites, were performed placing the samples inside dialysis membranes, and again, at predetermined time intervals, an aliquot of the liquid media was read in the UV-VIS spectrophotometer. For SNPs, every 24h the release media was replaced by fresh Milli-Q water, and after 72h, samples were leached out until no drug could be detected. The analysis was performed in quadruplicate and results are the average and standard deviation of at least two samples. In the case of the loaded foams, UV reading was performed during one week and the analysis was performed in triplicate and results are the average and standard deviation of at least two samples. Release kinetics was characterized by Korsmeyer-Peppas [10], Short-time and Long-time [11] equations considering slab geometry.

3. Results

3.1 Thermal Characterization

Thermogravimetric analysis shows that the samples with 70%wt of PCL present a corresponding mass loss was of 71.2 ± 3.5 % of the total mass. When concerning 90:10%wt samples, the residual mass corresponded to 9.8% and processed PCL, PCL-powder and PCL-pellet showed mass losses of 99.7 ± 0.6 %. This means that apparently the physical mixture of SNP and PCL prior to $scCO_2$ assisted foaming was efficient, once the mass loss corresponds to percentage of polymer in each formulation. Additionally, FTIR-ATR and SEM-EDX reveal the presence of the silica and PCL in the final formulations.

While the supplier reports PCL melting temperature values around 56-64 ºC, SDT results (Figure 1) indicated different and higher values (~67-68 ºC). Considering the indicated standard deviations, no apparent change occurred in the melting temperatures of PCL pellets and powder, but $scCO_2$-assisted processing lowered the PCL foam melting temperature when compared with the unprocessed samples. This effect becomes more pronounced (65 ºC) for the higher processing pressure due to the formation of different lamellar thickness, as reported by [2, 4]. The incorporation of MCM-41 SNPs during the $scCO_2$ processing

also seems to induce a further decrease in PCL melting temperature [12] and melting enthalpies. PCL degradation temperatures remain almost constant for all processed samples despite a decrease in these values can be observed for samples containing higher MCM-41 SNPs amounts. This indicates that the process decreased the crystallinity of PCL and composites, as indicated by XRD results in Figure 2. In our case, the lack of intercalation between MCM-41 and PCL physical mixture will ease thermally induced melting and degradation. However, melting and degradation temperatures obtained are above the physiological temperature, making these materials suitable for biomedical applications. Additionally, it is possible to predict/control degradation rate through crystallinity, varying the operational conditions.

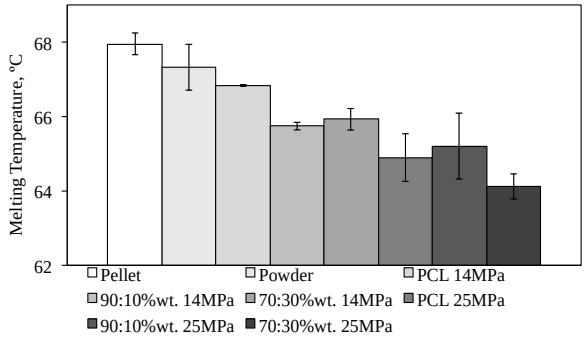

Figure 1. Melting temperature variation of PCL and composites processed for 2 h and 3.0 dm^3/min.

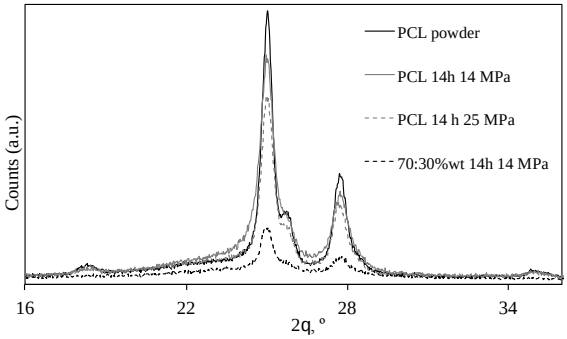

Figure 2. XRD diffractograms of — PCL powder, — PCL 14 h 14 MPa, --- PCL 14 h 25 MPa, --- 70:30%wt 14 h 14 MPa.

3.2 Foams Morphology

Samples density is mainly affected by the inorganic filler amounts, and as such, the increasing MCM-41 SNPs content led to higher density for all tested conditions, from 1.09 to 1.31 g/cm^3 within the range reported for bone tissue [13]. Increasing pressure slightly augments the density in 70:30%wt and 90:10%wt samples, while processing time and depressurization rate seem to have no strong effect on final sample density.

Regarding porosity, the major variable that affects this property is MCM-41 content while pressure does not have a clear effect, but the tendency is to slightly decrease the porosity with increasing pressure. Longer processing time tends to increase porosity once CO_2 sorption and polymer melting is enhanced for higher process times [14]. Depressurization rate seems to have no influence on the porosity of 70:30%wt composites, but for 90:10%wt and PCL foams (and both pressures) increasing depressurization rate led to a decrease in porosity. Nevertheless, the highest porosity value, ~55.4%, was found for 70:30%wt samples processed at high supercritical solvent density, regardless the remainder operational conditions, and the lowest was found for PCL samples processed at the same pressure (11.9%). The composites composed of an intermediate SNP composition show, once again, intermediate values.

Mercury intrusion revealed that rapid depressurization and higher pressure led to the decrease of the pore diameter, contrarily to slow depressurization rate which allows the formation of larger pores in the final construct, due to the gas diffusion rate in the liquefied polymer [1, 3].

It can be observed by SEM pictures (Figures 3) that different process conditions originated distinct porous morphologies. In general, increasing silica content led to large pores up to a certain amount of SNPs (10%) and above this silica composition pore diameter value decreased, a result also obtained by nitrogen adsorption and reported by other authors [15]. In 70:30%wt samples it is not possible to see pores due to their extremely small size; in 90:10%wt materials is possible to observe pores with diameters from approximately 50 μm up to pore diameters larger than 500 μm. PCL processed material presents pore diameters from tens of micron up to 500 μm, while in some cases, for the presented magnification, it seems that there are no pores but these can be inferior to 20 μm. Concluding, it is possible to achieve a wide range of pore sizes and morphology that are suitable for new tissue formation. This shows that, besides silica quantity, the predominant effect is CO_2 density/pressure, and depressurization rate stands out as an important parameter when a 10%wt of SNPs is used. As more SNPs are introduced, more nucleation points will be created and thus the number of growing bubbles will be larger (for the same amount of dissolved $scCO_2$) and the resulting pore dimensions will be smaller [16].

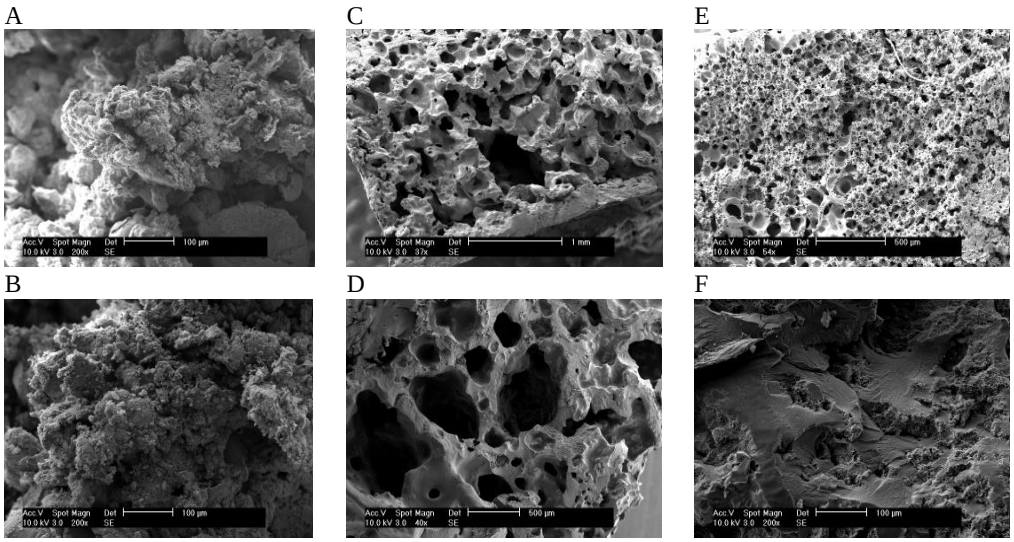

Figure 3. SEM micrographs for samples processed at 14 MPa and for 14 h. (A) PCL+30wt.% MCM-41 3 dm^3/min (B) PCL+30wt.% MCM-41 0.2 dm^3/min (C) PCL+10wt.% MCM-41 3 dm^3/min (D) PCL+10wt.% MCM-41 0.2 dm^3/min (E) Pure PCL 3 dm^3/min (F) Pure PCL 0.2 dm^3/min. The scale bar is indicated in each picture.

3.3 Mechanical Properties

Variations in mechanical resistance can be observed (Figure 4) mostly due to the filler content and the obtained results, especially for 90:10%wt samples, are similar to previous studies with other composite materials [17, 18]. The mechanical compression results were calculated at a 10% strain, and suggest that higher compressive stress (from 16±3 to 9±5 MPa) and moduli (from 164 to 60 MPa) were obtained for samples containing an intermediate amount of SNPs, despite the processing conditions. However, these values are still inferior to trabecular bone, reported as approximately 0.3 GPa for compressive modulus [17]. In the case of higher silica amounts (30%), the constructs become brittle and lower stress and modulus are obtained, and PCL samples also exhibit unsuitable mechanical properties.

Increasing porosity conduced to a decrease of moduli and stress as predicted by Gibson and Ashby model [18]; however, pure PCL samples (with the lowest values of porosity) also presented low mechanical properties, resulted from internal architecture incongruences. $ScCO_2$-foaming and a small quantity of SNPs originated materials with improved mechanical properties and satisfactory morphological features for bone tissue regrowth.

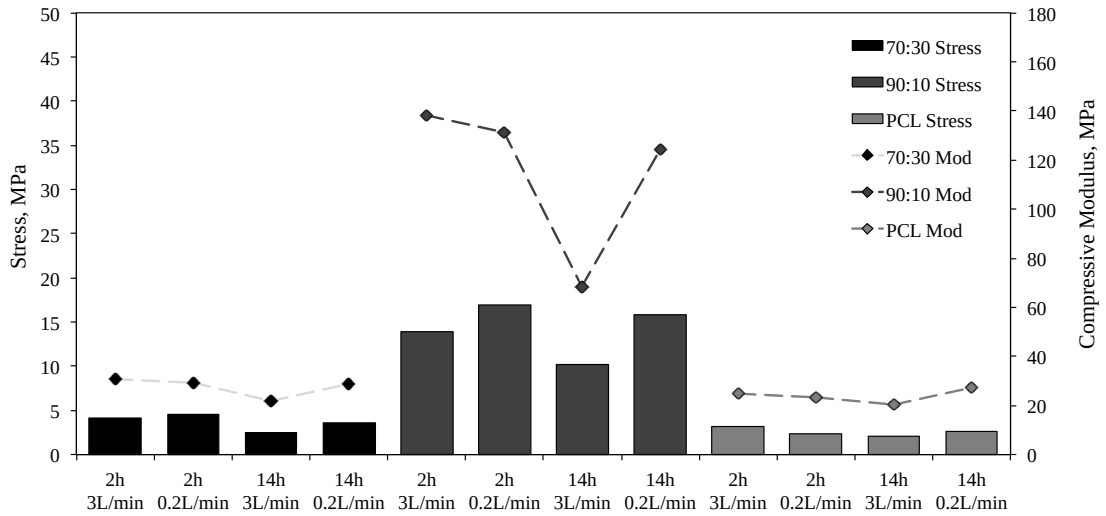

Figure 4. Compressive Stress and Modulus of samples processed at 25 MPa.

3.4 In Vitro drug release

Silica Nanoparticles. Dexamethasone was loaded into MCM-41 and SBA-15 by $scCO_2$ – assisted deposition and drug release studies were performed in order to analyze the effect of the process conditions. After 8h of DXMT release in milli-Q water it was found that, for all $scCO_2$-loading conditions, the amount of DXMT released was almost constant (approximately 1.5 and 3 μg/mg respectively, Figure 5). Complete leaching was used to ease diffusion and determine the total amount of DXMT that was still entrapped after 72 h of release (Figure 6). The differences between both SNPs in sorption and release results can be explained by SBA-15 physical properties because despite the slightly lower surface area, the pores are larger and the hydrophilicity is also high, which leads to an increased and faster drug adsorption capability. The total released value was also found to vary according to the employed pressure and processing time conditions, revealing that lower pressures and longer processing times appear to increase drug deposition yields and that faster drug release rates were obtained for those samples loaded at lower pressures. These results indicate that perhaps DXMT has a better affinity to the SNPs surface, rather than for the $scCO_2$ mobile phase, and even though the solubility in the latter is low [9], long-term release of DXMT is possible to achieve using supercritical CO_2 –assisted deposition.

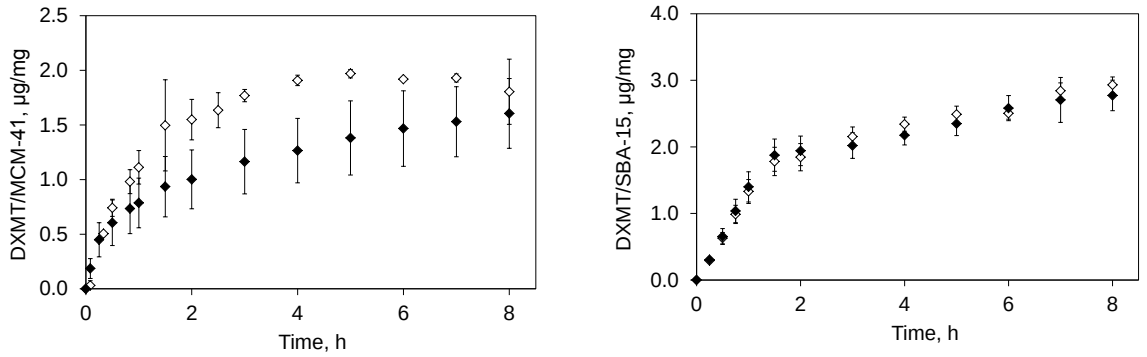

Figure 5. Dexamethasone 8 hour release profile from SNPs for supercritical CO2 assisted deposition at ◇14 MPa and ◆ 25 MPa and 14 h and slow depressurization.

PCL and Composites. PCL, PCL/MCM-41 and PCL/SBA-15 composites were loaded with 2%wt DXMT by $scCO_2$ mixing, and the profiles are represented on Figure 6. Considering the initial amount of DXMT, the amount released from PCL and composites is according to the general expected tendency, that is, higher released amounts for 70:30%wt and lower for PCL, while 90:10%wt remained with an intermediate value. The composites with higher quantity of SNPs, as previously discussed, have higher porosity and surface areas, and also more quantity of drug due to higher amount of loaded-SNPs and less PCL-slow degrading hydrophobic matrix, leading to this behavior.

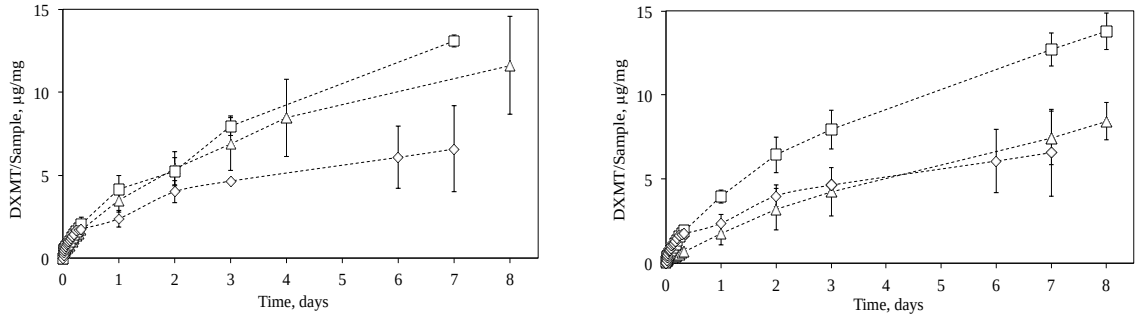

Figure 6. Dexamethasone 1 week release profile from ◇ PCL, △ 90:10%wt and □ 70:30%wt at 14 MPa for 14 h scCO2 – assisted foaming mixing. MCM-41 composites left figure, SBA-15 composites right figure.

The kinetic parameters indicate that supercritical foaming/mixing is a tunable process. In all cases, increasing pressure the release rate increases, mostly due to the morphologic characteristics induced by this experimental condition. Considering slab geometry, for PCL and 90:10%wt (PCL/SBA-15) samples processed at higher pressure, $n<0.5$ and thus the release mechanism is controlled by Fick diffusion. The remainder composites have $n>0.5$, which accounts for anomalous (non-Fickian) behavior that implies that drug release is a superposition of Fickian and case-II transport, and is probably due to the crystallinity (already seen to decrease with increasing pressure and SNPs quantity) and initial polymer surface erosion [10].

Release rate differences may be attributed to different morphologies, different drug available sites due to different pore sizes, porosities, surface areas [6], and possibly different host dissolution rates provided by SNPs amount and $scCO_2$ operational conditions already discussed in morphology results. Thus, for pure PCL the effect of pressure in both diffusion coefficients (D_1 and D_2) is not significant, but in the composites the higher the pressure, the higher the D_1 and D_2. Another parameter influencing the diffusion rate is the amount of SNPs; the increase of SNPs quantity from 10 to 30%wt caused a D_1 increase of ~85%, and a similar tendency is observed for D_2. As well, the SNP type in the composite seems to have an effect on diffusion coefficients: 70:30%wt composites from SBA-15 present a significantly higher D_1 rather than D_2, also confirmed by higher k, suggesting substantially higher rate and amount of drug released during the first period, while the opposite trend ($D_2 > D_1$) was obtained for the remaining composites. This result suggests that the more hydrophilic character of SBA-15, compared with MCM-41, combined with the morphology obtained at higher pressure, can indeed control DXMT release.

Because the release time was too short so that all DXMT was released, it is expected that a mechanically reinforced matrix developed from pre-loaded SNPs and semi-crystalline PCL continue to release the osteogenic and anti-inflammatory incorporated drug in a controlled way, contributing to the intended long-term hard-tissue application. Although the biocompatibility was not tested in this work, there are evidences that these materials are physiologically accepted and used for tissue engineering and/or drug delivery [19, 20].

4. Conclusions

The realization of this work presupposed the fabrication of PCL and PCL/SNPs scaffolds loaded with dexamethasone through supercritical fluids, a green technology process. The main goals were attained once PCL/SNPs biodegradable scaffolds were produced and successfully loaded with DXMT, several working parameters where varied and studied, and distinct profiles were obtained. Thus, chemically PCL and its composites presented no alteration induced by processing with $scCO_2$. Also, PCL and its PCL/MCM-41 composites showed thermic characteristic that allow them to be used in the physiological media. Regarding crystallinity, strongly related to degradability and drug release rates, was found to be tunable. Pore sizes and porosities were found to be appropriate for hard tissue engineering application. The best morphology and with the most suitable mechanical properties for tissue regrowth seams to occur in samples with 10%wt of MCM-41 when processed at 25 MPa with low depressurization rate, and 14 MPa for 2 h and low depressurization rate. Regarding drug loading, varying the working conditions can easily change process yields. PCL and PCL/SNPs systems presented a sustained release profile, contrarily to SNPs (both MCM-41 and SBA-15) that show burst release. Therefore, the main purpose of this work was accomplished. Supercritical CO_2 was successfully and easily used to create drug-eluting systems based on PCL and silica nanoparticles with distinct release profiles.

Additionally, $scCO_2$ technology allows different routes for industrial processing, such as extrusion and injection molding, which will in due course define the application, that may be grind and integrated in a hydrogel or in bone cement.

Acknowledgements

Authors are also thankful to Programa CYTED - Ciência y Tecnologia para el Desarrollo under the scope of the Red Iberoamericana de nuevos materiales para el diseño de sistemas avanzados de liberación de fármacos en enfermedades de alto impacto socioeconómico (RIMADEL).

References

[1] H. Tai, V.K. Popov, K. M. Shakesheff, S. M. Howdle, Putting the fizz into chemistry: applications of supercritical carbon dioxide in tissue engineering, drug delivery and synthesis of novel block copolymers, Biochemical Society Transactions 35 (2007) 516-521.

[2] Y.-T. Shieh, J.-G. Lai, W.-L. Tang, C.-H. Yang, T.-L. Wang, Supercritical CO_2 intercalation of polycaprolactone in layered silicates, Journal of Supercritical Fluids 49 (2009) 385–393.

[3] Q. Xu, X. Ren, Y. Chang, J. Wang, L. Yu, K. Dean, Generation of microcellular biodegradable polycaprolactone foams in supercritical carbon dioxide, Journal of Applied Polymer Science 94 (2004) 593–597.

[4] A. Léonard, C. Calberg, G. Kerckhofs, M. Wevers, R. Jérôme, J. Pirard, A. Germain, S. Blacher, Characterization of the porous structure of biodegradable scaffolds obtained with supercritical CO_2 as foaming agent, Journal of Porous Mater 15 (2008) 397–403.

[5] R.J. Ahern, A. M. Crean, K. B. Ryan, The influence of supercritical carbon dioxide (SC-CO_2) processing conditions on drug loading and physicochemical properties. Int J Pharmaceut 439 (2012) 92–99.

[6] M. E. M. Braga, M. V. Pato, H. S. R. C. Silva, E. I. Ferreira, M. H. Gil, C. M. M. Duarte, H. C. de Sousa, Supercritical solvent impregnation of ophthalmic drugs on chitosan derivatives, Journal of Supercritical Fluids 44 (2008) 245–257.

[7] A. López-Periago, A. Argemí, J. M. Andanson, V. Fernández, C. A. García-González, S. G. Kazarian, J. Saurina, C. Domingo, Impregnation of a biocompatible polymer aided by supercritical CO2: Evaluation of drug stability and drug–matrix interactions, Journal of Supercritical Fluids 48 (2009) 56–63.

[8] C.-H. Kim, S-L Cheng, G. S. Kim, Effects of dexamethasone on proliferation, activity, and cytokine secretion of normal human bone marrow stromal cells: possible mechanisms of glucocorticoid-induced bone loss, Journal of Endocrinology 162 (1999) 371–379.

[9] R.B. Chim, M. B. C. de Matos, M.E.M. Braga, A.M.A. Dias, H.C. de Sousa, Solubility of dexamethasone in supercritical carbon dioxide, Journal of Chemical & Engineering Data, 57 (2012) 3756–3760.

[10] J. Siepmann, N.A. Peppas, Modeling of drug release from delivery systems based on hydroxypropyl methylcellulose (HPMC), Advanced Drug Delivery Reviews 48 (2001) 139–157.

[11] J. Siepmann, F. Siepmann, Modeling of diffusion controlled drug delivery, J. Control. Release, 161 (2011) 351–362.

[12] A. Salerno, E. Di Maio, S. Iannace, P.A. Netti, Solid-state supercritical CO_2 foaming of PCL and PCL-HA nano-composite: Effect of composition, thermal history and foaming process on foam pore structure, J. of Supercritical Fluids 58 (2011) 158–167.

[13] P. Zioupos, R. B. Cook, J. R. Hutchinson, Some basic relationships between density values in cancellous and cortical bone, Journal of Biomechanics 41 (2008) 1961–1968.

[14] M. A. Fanovich, P. Jaeger, Sorption and diffusion of compressed carbon dioxide in polycaprolactone for the development of porous scaffolds, Materials Science and Engineering C, 32 (2012) 961–968.

[15] N. J. Collins, G. A. Leeke, R. H. Bridson, F. Hassan, L. M. Grover, The influence of silica on pore diameter and distribution in PLA scaffolds produced using supercritical CO_2, Journal of Materials Science: Materials in Medicine 19 (2008) 1497–1502.

[16] W. Zhai, J. Yu, L. Wu, W. Ma, J. He, Heterogeneous nucleation uniformizing cell size distribution in microcellular nanocomposites foams, Polymer 47 (2006) 7580-7589.

[17] G. Georgiou, L. Mathieu, D. P. Pioletti, P.-E. Bourban, J.-A. E. Månson, J. C. Knowles, S. N. Nazhat, Polylactic acid-phosphate glass composite foams as scaffolds for bone tissue engineering, J Biomed Mater Res Pt B Appl Biomater 80 (2007) 322-331.

[18] L. M. Mathieu, M.-O. Montjovent, P-E. Bourban, D. P. Pioletti, J.-A. E. Månson, Bioresorbable composites prepared by supercritical fluid foaming, Journal of Biomedical Materials Research Part A 75 (2005) 89-97.

[19] C. Fruijtier-Pölloth, The toxicological mode of action and the safety of synthetic amorphous silica—A nanostructured material, Toxicology 294 (2012) 61–79.

[20] J.-T. Schantz, D. W. Hutmacher, C. X. F. Lam, M. Brinkmann, Wong K. M., Lim T. C., Chou N., Guldberg R. E., Teoh S. H. Repair of Calvarial Defects with Customised Tissue-Engineered Bone Grafts II. Evaluation of Cellular Efficiency and Efficacy *in Vivo*. Tissue Engineering 9 (2004) 127-139.